sciendo

Nova Biotechnol Chim (2018) 17(1): 16-28
DOI: 10.2478/nbec-2018-0002

Nova Biotechnologica *et* Chimica

Adsorptive removal of ciprofloxacin and isoniazid from aqueous solution

Cyril Dube[1], Roman Tandlich[1,✉] and Brendan Wilhelmi[2]

[1]*Environmental Health and Biotechnology Research Group, Division of Pharmaceutical Chemistry, Faculty of Pharmacy, Rhodes University, Grahamstown, 6140, South Africa*
[2]*Department of Biochemistry and Microbiology, Rhodes University, 6140, South Africa*

Article info

Article history:
Received: 1st April 2018
Accepted: 20th June 2018

Keywords:
Adsorption
Ciprofloxacin
Isoniazid
Wastewater
Antimicrobial resistance

Abstract

This paper describes study of ciprofloxacin and isoniazid removal from aqueous solutions using coal fly ash (FA), kaolinite, perlite, talc and vermiculite. The adsorptive features of the adsorbents were evaluated for ciprofloxacin and isoniazid with regards to the effects of contact time, pH, the solid/liquid ratio and antibiotic concentration. All adsorbents were sterilised by dry heat before use to avoid the proliferation of antimicrobial resistance by the bacteria present on the adsorbents during experiments. The regression correlation coefficients indicate that the Langmuir model gives the best fit for the sorption of both antibiotics onto FA and talc, ciprofloxacin onto kaolinite, and isoniazid onto perlite and vermiculite with R^2 values ranging from 0.908 – 0.999. The Freundlich isotherm best describes the sorption of ciprofloxacin onto vermiculite and isoniazid onto kaolinite with R^2 values of 0.999 for both. The Tempkin model best describes the sorption of ciprofloxacin onto perlite with an R^2 = 0.997. The values of the Freundlich exponent, 1/*n*, range from 0.221 – 0.998, indicating a favourable adsorption of ciprofloxacin and isoniazid onto the adsorbents. The heat of sorption, B, calculated from the Temkin plots has values ranging from 0.018 – 10.460 J/mol, indicating a physical adsorption process (physisorption). Adsorption equilibrium was achieved after 30 min for both antibiotics and the kinetic data obtained conforms best to the pseudo-second order equation with R^2 values ranging from 0.998 – 0.999. The removal of ciprofloxacin and isoniazid by all adsorbents except FA was strongly influenced by the pH suggesting that electrostatic interactions play a major role in the adsorption processes.

Introduction

The prevailing emergence of antimicrobial resistance amongst bacteria remains a serious health and economic problem. It is estimated that about 700 000 deaths occur worldwide every year as a result of antibiotic resistance (Bengtsson-Palme and Larsson 2016). Antibiotics are extensively used worldwide in human and veterinary medicine for therapeutic, prophylactic and growth enhancing purposes (Chen *et al.* 2016). Consequently, they are relentlessly discharged into the environment and are therefore considered to be "pseudo-persistent" environmental pollutants (Yao *et al.* 2015). Antibiotics in wastewater from domestic, hospital, farm and industrial effluent (Wu *et al.* 2016) are released into wastewater treatment plants (WWTP) which act as the major port of entry of antibiotics into different facets of the environment (Luo *et al.* 2014).

✉ *Corresponding author:* r.tandlich@ru.ac.za

The application of adsorption technology to remove wastewater pollutants has proven to be one of the most versatile water treatment methods which is efficient, environmentally friendly and easy to operate (Yu *et al.* 2016). Naturally occurring rock minerals such as kaolinite, perlite, talc and vermiculite and waste-derived materials such as coal fly ash (FA), a mineral residue, are potential alternatives owing to their porous nature, chemical inertness, relatively low costs and availability in commercially bulk quantities (Ahmaruzzaman 2010; Kolvari *et al.* 2015; Tian *et al.* 2016). In the present study, the removal of ciprofloxacin and isoniazid from aqueous media by sorption onto kaolinite, perlite, talc, vermiculite and FA in a batch system was investigated. The adsorption of antibiotics at the solid–liquid interface is strongly influenced by the nature of the structural groups present on the solid surface, the molecular structure of the antibiotic being adsorbed and the environment of the aqueous phase. Therefore, the effect of varying parameters such as the solid/liquid ratio, pH, contact time, initial antibiotic concentration was also investigated. Langmuir, Freundlich and Temkin isotherms were used to analyse the data.

Experimental

Reagents and chemical

Ciprofloxacin (purity ≥ 98%, CAS # 85721-33-1) and isoniazid (purity ≥ 99%, CAS # 54-85-3) were purchased from Sigma-Aldrich (Pty.) Ltd. (Johannesburg, RSA). All other chemicals were of analytical grade and were used as received without any further purification. MilliQ water was obtained from a Milli-Q® RiOs™ and Academic A10 Water Purification system (Merck Millipore, Bedford, USA). FA was obtained from Ash Resources (Pty.) Ltd. (Randburg, RSA). Ground talc was purchased from Micronized Products (Pty.) Ltd. (Johannesburg, RSA). Raw kaolinite was obtained from the local Strowan Mine (Grahamstown, RSA). Perlite and vermiculite, both in the expanded form, were obtained from Sunshine Nursery (Grahamstown, RSA).

Preparation and characterization of adsorbents

The adsorbents were ground using a mortar and pestle and passed through a 0.315 µm mesh sieve to ensure uniform particle size. Afterwards, the adsorbents were washed with MilliQ water, in the ratio 1:10 (g/mL), by stirring on a model STR-MH magnetic stirrer (FMH Laboratory Products, RSA) at speed 5 for 24 hours. The suspensions were then separated by vacuum filtration and dried for 12 hours in a Memmert ULM600 oven (Memmert, Western Germany) at 105 ^{o}C. All adsorbents and glassware were sterilised by dry heat at 160 ^{o}C and left to air dry for 24 hours in an LA-1200 BII Laminar-flow hood (Vivid Air, RSA).

Characterization of the adsorbents was done by determining the pH, cation exchange capacity (CEC) using the ammonium acetate saturation method (Sumner and Miller, 1996), specific surface area (SSA) using the ethylene glycol monomethyl ether (EGME) method (Tandlich and Balaz 2011), total organic carbon content using the loss on ignition (LOI) method (Salehi *et al.* 2011), surface morphology was observed on a Tescan VEGA LMU scanning electron microscope (SEM) (Tescan, Czechoslovakia), mineralogical composition using (XRD) patterns were recorded using a Bruker D8 Discover machine (Bruker, Germany) equipped with the PSD Lynx Eye detector, using Cu-K radiation (λ = 1.5405 Å, nickel filter). The Fourier transform infrared (FTIR) spectra were obtained at room temperature from an average of 10 individual scans using Perkin Elmer version 10.4 spectrophotometer (Perkin Elmer, Port Elizabeth, South Africa) in the spectral range of 4,000 to 650 cm^{-1} having a resolution of 4 cm^{-1} by the KBr disc method. Furthermore, XRD patterns and FTIR spectra were used to investigate the adsorption mechanisms.

Adsorption Studies

All adsorption experiments were carried out by the batch equilibration method at room temperature (25±1 ^{o}C) in duplicates. Aqueous stock solutions of concentration 1.0 g/L were prepared by dissolving the antibiotic powders in MilliQ water. In the adsorption kinetics studies,

0.1 ± 0.001 g and 1.0 ± 0.01 g were added to sterile 30 mL centrifuge tubes containing 10 mL ciprofloxacin and isoniazid solution, respectively. The concentration of the antibiotic which was obtained from the dilution of the stock solutions was 25 mg/L. The mixtures were shaken on a Junior Orbit Shaker (LAB-LINE Instruments Inc., Melrose Park, ILL) at a constant speed of 220 rpm for a fixed time interval (5, 10, 15, 30, 60, 120, 240 and 480 min) in the dark. After shaking, the mixtures were separated by centrifugation on a Mixtasel centrifuge (Selecta®, Barcelona, Spain) at 700 RCF for 10 min and passing the supernatants through a 0.45 µm syringe filter. Antibiotic solutions which were not mixed with adsorbents were used as controls to assess the influence of phase separation on the initial antibiotic concentrations. The filtrates were then diluted accordingly with MilliQ water. The concentrations of the antibiotic solutions were determined spectrophotometrically using a Cintra 10 GBC 916 UV/VİS spectrophotometer (GBC Scientific Equipment (Pty) Ltd., Melbourne, Australia) wavelengths of maximum absorbance, 277 nm and 262.5 nm for ciprofloxacin and isoniazid, respectively. The wavelengths of maximum absorbance of the antibiotics were predetermined spectrophotometrically after eliminating the background influence of the aqueous phase by performing an automatic baseline correction with a blank solution. Calibration curves were established by using ten standards in the range 0 to 7.5 mg/L and 0 to 27 mg/L for ciprofloxacin and isoniazid, respectively.

To investigate the effects of the solid/liquid ratio on antibiotic sorption, dosages of 0.100, 0.175, 0.250 g were used for ciprofloxacin solutions and 0.5, 1.0 and 1.5 g were used for isoniazid solutions. Influence of pH was evaluated by adjusting the initial pH of the antibiotic solutions ranging from 3 to 12 using 0.1 M aqueous solutions of HCl or NaOH.

To obtain adsorption isotherms, solutions of different antibiotic concentrations (5 – 250 mg/L) were made by diluting the stock solutions with MilliQ water. The ciprofloxacin and isoniazid solutions were mixed with 0.1 ± 0.001 g and 1.0 ± 0.01 g adsorbent, respectively. The mixtures were shaken at 220 rpm for 40 min to allow adsorbents to reach equilibrium adsorption. The initial pH of antibiotic solutions was at the optimum for maximum adsorption for each adsorbent. The amounts of antibiotic adsorbed and % removal were calculated by mass balance using the formula (Eq. 1 and 2):

$$q_e = \frac{C_o - C_e}{w} V \quad (1)$$

$$\%\ removal = \frac{C_o - C_e}{C_o}\ x\ 100 \quad (2)$$

where q_e (mg/g) is the amount of antibiotic adsorbed at equilibrium, w (g) is the weight of the adsorbent, V (L) is the volume of antibiotic solution, C_o (mg/L) is the initial antibiotic concentration in solution and C_e (mg/L) is the concentration of antibiotic remaining in solution at equilibrium.

Results and Discussion

Characterization

Physicochemical properties of sorbents

The physical-chemical properties of adsorbents are important parameters in adsorption processes and are often manipulated to enhance the adsorption process. The physicochemical properties of the adsorbents are shown in Table 1. Most of the values are in agreement to those reported in literature; specific surface area (SAA) of talc and kaolinite (Ouchiar *et al.* 2015), cation exchange capacity (CEC) of vermiculite (Sutcu 2015), pH of vermiculite (Rashad 2016a), pH of perlite (Rashad 2016b), CEC and SAA of perlite (Tekin *et al.* 2010), CEC of FA (Visa 2016), SAA of FA and CEC of talc (Dellisanti *et al.* 2009).

Table 1. Physicochemical properties of adsorbents.

Adsorbent	pH	CEC [cmol/kg]	SAA [m^2/g]	Average LOI [%]
FA	12.2	9.46	5.5	0.60
Talc	8.6	12.02	6.3	0.16
Perlite	5.3	41.21	3.1	0.86
Kaolinite	7.6	15.15	20.2	0.47
Vermiculite	7.5	86.52	5.9	0.20

Effect of contact time on antibiotic sorption

Contact time is a very important parameter that influences the effectiveness of the adsorption process. The adsorption is almost instantaneous and increased sharply initially, after which it slows as it approaches a state of adsorption equilibrium after 30 min. This is because initially, the sorbent sites are vacant resulting in a higher frequency of interactions between the sites and antibiotic molecules. As time lapses the sorption sites continue getting occupied and gradually most sites become saturated. The few if any remaining vacant sites become more difficult to occupy due to repulsive forces between the antibiotic molecules on the surface of the adsorbent and those in the bulk solution (Singh and Choden 2014). The highest rate and extent of adsorption of both ciprofloxacin and isoniazid are exhibited by kaolinite. Whereas, vermiculite and FA show both the lowest rate and extent of adsorption of isoniazid and ciprofloxacin, respectively. Adsorption equilibrium for isoniazid and ciprofloxacin was achieved in 30 min by all adsorbents and was kept at 40 min for the rest of the experiments.

Table 2. Kinetic parameters for adsorption of ciprofloxacin onto FA, kaolinite, perlite, talc and vermiculite. Derived from pseudo-first-order, pseudo-second order and intraparticle diffusion models.

	Pseudo-first order			Pseudo-second order			Intraparticle diffusion		
Adsorbent	K_1 [min^{-1}]	$q_{e.c}$ [mg/g]	R^2	K_2 [mg/g.min]	$q_{e.c}$ [mg/g]	R^2	K_{id} [mg/g.$min^{0.5}$]	C [mg/g]	R^2
FA	0.1870	0.3309	0.9945	0.9343	0.9319	0.9999	0.0650	0.6190	0.9889
Talc	0.1803	0.3351	0.9719	0.9649	1.8875	0.9999	0.0776	1.5300	0.9222
Perlite	0.0829	0.2037	0.9943	1.4248	1.1375	0.9997	0.0454	0.9194	0.9989
Kaolinite	0.1819	0.2735	0.9776	1.3500	2.2341	0.9999	0.0521	1.9875	0.9996
Vermiculite	0.2006	0.2979	0.9842	1.2110	1.9662	0.9999	0.0635	1.6744	0.9270

Adsorption kinetics

The non-equilibrium stages of adsorption were used to make a kinetic evaluation of the adsorption behaviours of ciprofloxacin and isoniazid by the adsorbents. The adsorption rate constants were estimated using the linearised forms of the following kinetic models based on the R^2 values and amount of antibiotic adsorbed per unit weight of adsorbent. The pseudo first-order rate model expressed as (Eq. 3, 4 and 5):

$$\log(q_e - q_t) = \log q_e - \left(\frac{k_1}{2.303}\right)t \quad (3)$$

The second-order rate model expressed as:

$$\frac{t}{q_t} = \frac{1}{k_2 q_e^2} + \left(\frac{1}{q_e}\right)t \quad (4)$$

The intra particle diffusion model is expressed as:

$$q_t = k_{id}t^{0.5} + C \quad (5)$$

where q_e and q_t (both in mg/g) are the amounts of antibiotic adsorbed per unit mass of adsorbent at equilibrium and time t (min), respectively, k_1 (min^{-1}) is the rate constant of the pseudo-first-order model, k_2 (mg/g.min) is the rate constant of the pseudo-second-order model, k_{id} (mg/g.$min^{0.5}$) is the rate constant of the intra-particle diffusion model. Values of k_1 and q_e can be calculated from the slope and intercept of the linear plot of log $(q_e - q_t)$ versus t, respectively. Values of k_2 and q_e can be calculated from the intercept and slope of the linear plot of t/q_t versus t, respectively. The value of k_{id} can be calculated from the slope the linear plot q_t versus $t^{0.5}$ and C (mg/g) is the intercept (Nithya *et al.* 2016). Parameters and regression coefficients for the treatment of ciprofloxacin and isoniazid data according to each kinetic equation are presented in Table 2 and Table 3, respectively.

Based on the R^2 values, the pseudo-second-order model gives the better fit for the adsorption of both ciprofloxacin and isoniazid onto all the adsorbents, with R^2 values ranging from 0.9987-0.9999, compared to the pseudo-first and intra-particle diffusion model. The data of equilibrium adsorbed amount calculated from the pseudo-second-order kinetics ($q_{e.c}$) are also close to the amounts adsorbed at equilibrium in experiments. This suggests that the sorption of ciprofloxacin

and isoniazid obey pseudo-second order kinetics. It is interesting to note that when employing the pseudo-first order model, close to equilibrium the value of q_t approaches q_e resulting in q_e-q_t becoming smaller and smaller. Ln q_e-q_t takes very large and uncertain values compromising the fit

Table 3. Kinetic parameters for adsorption of isoniazid onto FA, kaolinite, perlite, talc and vermiculite. Derived from pseudo-first-order, pseudo-second order and intraparticle diffusion models.

	Pseudo-first order			Pseudo-second order			Intraparticle diffusion		
Adsorbent	K_1 [min^{-1}]	$q_{e.c}$ [mg/g]	R^2	K_2 [mg/g.min]	$q_{e.c}$ [mg/g]	R^2	K_{id} [$mg/g.min^{0.5}$]	C [mg/g]	R^2
FA	0.1630	0.0527	0.9677	5.2455	0.1374	0.9987	0.0105	0.0857	0.9984
Talc	0.1370	0.0201	0.9830	12.052	0.0503	0.9986	0.0044	0.0287	0.9997
Perlite	0.1745	0.0387	0.9859	6.0785	0.0693	0.9990	0.0077	0.0287	0.9980
Kaolinite	0.1361	0.0594	0.9960	4.0844	0.1555	0.9995	0.0134	0.0899	0.9973
Vermiculite	0.1671	0.0161	0.9974	12.782	0.0273	0.9998	0.0034	0.0100	0.9894

of the model. On the other hand, the pseudo-second-order gives a more accurate fit of the experimental data with giving almost perfect R^2 values because in the plots when the majority of the data is at equilibrium the data points are well aligned because the value of $t/q_t \simeq t/q_e$ when $q_t \simeq q_e$ (Simonin 2016).

Interaction between the antibiotics and the sorbent surfaces

The SEM images of the adsorbents indicated that characteristics of all sorbents were similar to what is reported in literature (Hongo *et al.* 2012; Sprynskyy *et al.* 2011; Zhang *et al.* 2017). Results of the XRD analyses indicated that the crystalline structure of FA and kaolinite was affected by the sorption of ciprofloxacin and isoniazid. Crystaline structure of perlite and talc was not affected by the sorption of either of the two antibiotics. Both antibiotics could have been intercalated between the inner layers of vermiculite.

FTIR spectral analysis can be used to identify specific functional groups present within the Si-containing or crystalline phases of the adsorbents. This assists in understanding the adsorption mechanisms and interactions between the antibiotics and the adsorbents. The IR spectra of the adsorbents are presented in Fig. 1. FA has a heterogeneous structure consisting of a glassy surface layer (SiO_2) and crystalline components such as quartz, mullite and magnetite. Hence, its FTIR (Fig. 1A) exhibits a broad band in the range 1,200 – 900 cm^{-1} with a centre around 1,090 cm^{-1} which is attributed to the asymmetric stretching vibration peaks of Si-O-Si or Si-O-Al bonds of SiO_2 or AlO_4 tetrahedrons which overlap in this region (Böke *et al.* 2015; Onutai *et al.* 2016). The shoulder visible between 1,074 and 1,069 cm^{-1} corresponds to the Si-O-Si stretching vibration. After shaking with the ciprofloxacin and isoniazid solutions, the peak of the centre of the broad band corresponding crystalline structure of FA shifted to lower wavenumbers around 1,080 and 1,060 cm^{-1}, respectively. This indicates a possible interaction of the oxygen with the antibiotics resulting in a greater number of non-bridging oxygen atoms (Shearer *et al.* 2016). The bands at 3,340 and 1,635 cm^{-1} are respectively assigned to the O-H stretching and bending of absorbed water indicating the presence of the antibiotic molecules on the surface of the adsorbent (Timakul *et al.* 2016; ul Haq *et al.* 2014).

The IR spectra of kaolinite (Fig. 1B) reveal that raw kaolinite exhibits bands in the range 3,694 – 3,620 cm^{-1} corresponding to stretching vibrations of OH groups coordinated to Al^{3+} ions. The peaks at 3,694, 3,672 and 3,620 cm^{-1} exhibited on FTIR spectra of kaolin are assigned to the in-phase stretching vibrations of inner surface OH groups. The peak at 3,654 cm^{-1} is attributed to the out of phase stretching of inner O-H groups (Zhu *et al.* 2016). All three peaks are also present in the spectra of kaolin after shaking with both antibiotic solutions indicating that no intercalation took place, instead, hydrogen bonding or ligand exchange might have occurred on the external surface of kaolinite (Spence and Kelleher 2012).

Intercalation would have resulted in the reduction of electrostatic attractive forces between the antibiotics and the inner surface OH groups of the layers thus separating them (Castrillo *et al.* 2015). The bands around 3,400 and 1,650 cm^{-1} correspond to stretching and bending vibrations of water molecules, respectively. The peaks at 933 and 908 cm^{-1}, which are attributed to Al-OH deforming vibration and Al-OH bending vibration move to higher wave number and an increase in intensity (Zhu *et al.* 2016). The presence of quartz in the kaolinite used is revealed by the low-intensity doublet with bands at 798 and 780 cm^{-1} (Król *et al.* 2016).

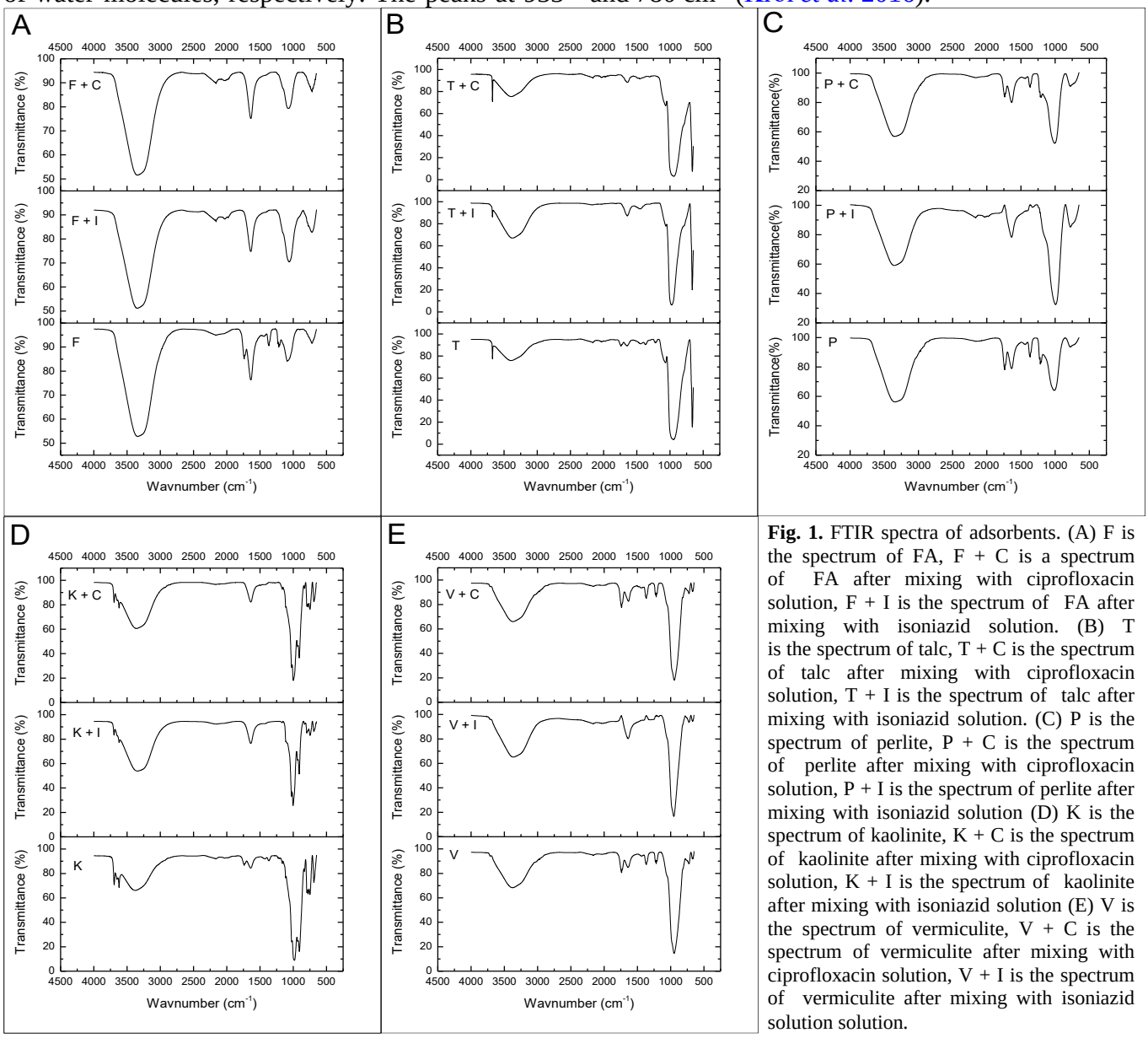

Fig. 1. FTIR spectra of adsorbents. (A) F is the spectrum of FA, F + C is a spectrum of FA after mixing with ciprofloxacin solution, F + I is the spectrum of FA after mixing with isoniazid solution. (B) T is the spectrum of talc, T + C is the spectrum of talc after mixing with ciprofloxacin solution, T + I is the spectrum of talc after mixing with isoniazid solution. (C) P is the spectrum of perlite, P + C is the spectrum of perlite after mixing with ciprofloxacin solution, P + I is the spectrum of perlite after mixing with isoniazid solution (D) K is the spectrum of kaolinite, K + C is the spectrum of kaolinite after mixing with ciprofloxacin solution, K + I is the spectrum of kaolinite after mixing with isoniazid solution (E) V is the spectrum of vermiculite, V + C is the spectrum of vermiculite after mixing with ciprofloxacin solution, V + I is the spectrum of vermiculite after mixing with isoniazid solution solution.

For perlite (Fig. 1C), the band at 1,014 cm^{-1} of the perlite FTIR spectra represents Si-O-Si asymmetric stretching vibration (Sun and Wang 2015) which shifted to a lower wavenumber after shaking with the antibiotic solutions. This suggests that interaction occurred, and based on the abundance of hydroxyl groups that exist on the inner surface of perlite, possibly hydrogen bonding and electrostatic attraction occurred with the functional groups on the antibiotics. It is also noteworthy that the bands at 778 and 3,342 cm^{-1} are attributed to stretching of O-H and Si-OH respectively (Sun and Wang 2015), shifted to higher wavenumbers suggesting a reduction in bond strength possibly resulting from weaker electrostatic attractions between the perlite and both antibiotics. The peak

at 1,045 cm^{-1} is the characteristic absorption peak of the telescopic vibration of Si-O-Si, and the shift to lower wave number after shaking with the antibiotic solutions is attributed to hydrogen bonding (Wei *et al.* 2014).

For talc (Fig. 1D), the bands ranging between 3,700 – 3,400 cm^{-1} are attributed to the stretching vibrations of O-H associated with Si (Si-OH) and Mg (Mg-OH) (Sprynskyy *et al.* 2011). Characteristically, the band at 3,678 cm^{-1} is associated with O-H in the 3 Mg region (Mg_3-OH) of talc (Ngally Sabouang *et al.* 2015). This band showed a significant change decrease in intensity after shaking with isoniazid solutions and increase in intensity after shaking ciprofloxacin solutions, respectively. This strongly suggests a possible interaction of the Mg-OH with the antibiotics. The same explanation can be given for shifts of wavenumbers of the band at 664 cm^{-1} which is assigned to the O-H stretching vibrations associated with Mg-OH.

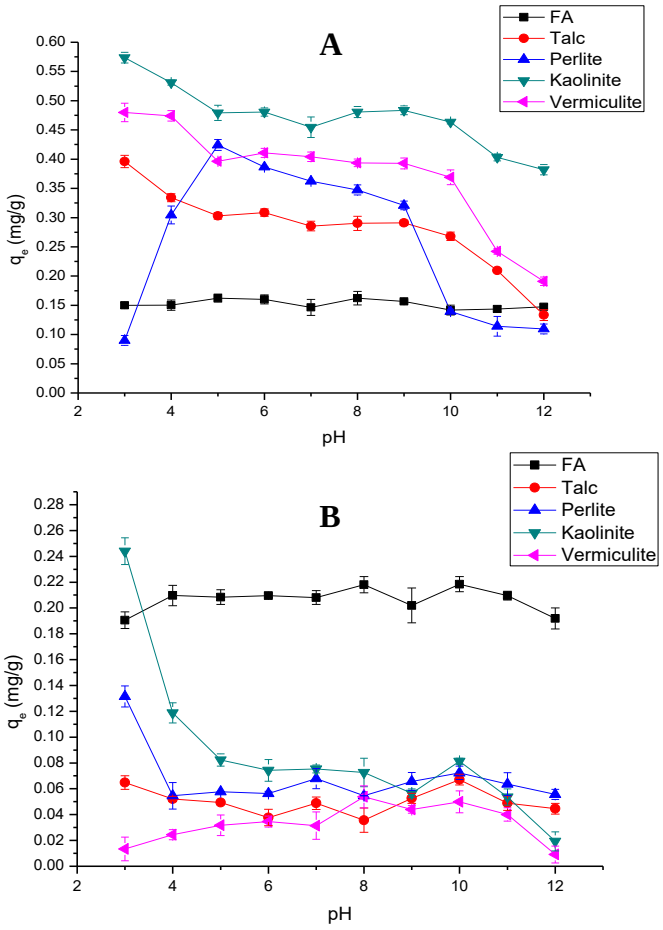

Fig. 2. Effect of pH on the adsorption of (A) ciprofloxacin and (B) isoniazid onto FA, kaolinite, perlite, talc and vermiculite. Amount adsorbed at equilibrium (q_e) presented as the mean ± standard deviation (n = 3).

A significant shift to lower wavenumbers and a marked increase in the intensity of the band at 3,400 cm^{-1} corresponding to Si-OH groups was observed after shaking with isoniazid solution. This is an expected binding site for isoniazid as the antibiotic is most likely to bind to surface hydroxyls by hydrogen interaction through ring nitrogen lone pairs directly, or indirectly through water bridges (Akyuz *et al.* 2010).

The IR spectra of vermiculite (Fig. 1E) show bands at 3,414 and 999 cm^{-1} which represent the O-H stretching vibrations of Si-OH groups and Si-O-Si groups of the silicate framework of vermiculite, respectively (Tran *et al.* 2015). The peak 1,637 cm^{-1} is attributed to the O-H bending vibration (Oliveira *et al.* 2015). Band at 999 cm^{-1} shifted to higher wavenumbers and there was an increase in the signal intensity after shaking with the antibiotic solutions which indicating interaction, between the sorbent and the antibiotic molecules. The peaks at 667 and 729 cm^{-1} which are attributed to the stretching vibrations of *X*-O-Si, where *X* = Mg, Al or Fe and Si-O & Al-O, respectively (Hongo *et al.* 2012), they also shifted to higher wavenumbers after shaking with the antibiotics solutions. The adsorption at 1,645 cm^{-1} is primarily due to water directly coordinated to the exchangeable cations of the clay (Tran *et al.* 2015). The significant shift of this band to lower wavenumber after shaking with ciprofloxacin suggests that cation exchange was one of the mechanisms of adsorption in the removal of ciprofloxacin by vermiculite.

Influence of pH

The adsorption mechanism is generally dictated by the physical and chemical interactions which occur between the adsorbate and adsorbent (Zhao *et al.* 2016). The presence of highly charged groups on the surfaces of all the adsorbents make them very sensitive to pH changes and this results in a significant influence on the degree of interaction between the antibiotics and adsorbents. The influence of pH on the removal of ciprofloxacin and isoniazid from aqueous solutions by FA, kaolinite, perlite, talc and vermiculite is depicted in Fig. 2.

There is a strong dependence on pH exhibited by the adsorption of ciprofloxacin and isoniazid by all adsorbents except FA. In general, the net surface charge of mineral oxides such as silica and alumina, tend to become more positive under acidic conditions i.e. when pH is lowered resulting in the adsorption of anionic species and decrease in the adsorption of cationic species (Alkan *et al.* 2005). However, looking at Fig. 2, most ciprofloxacin was adsorbed within the pH range 3-5 by all adsorbents except FA. In this pH range, pH < 5.90, ciprofloxacin predominantly exists as a cationic species as a result of the basic nitrogen in the piperazine ring being protonated to form a positively charged ciprofloxacin ion (pK_a 1). Under basic conditions, pH > 8.89, the carboxylic acid functional group is deprotonated to form an anionic species (pK_a 2). At neutral pH, 5.90 ≥ pH ≥ 8.89, ciprofloxacin occurs as a zwitterion (Chang *et al.* 2016; Nageswara Rao *et al.* 2008). This, therefore, suggests that cation exchange is the dominant mechanism of adsorption of ciprofloxacin by kaolinite, talc, perlite and vermiculite at lower pH values.

There is a significant drop in the adsorption of ciprofloxacin as pH approaches pK_a 1 indicating that the cation is no longer the dominant species. The general minimum variation in adsorption of ciprofloxacin that is observed at pH ≥ pK_a 1 suggests that the positive charge on the ciprofloxacin cation still contributes to adsorption via cation exchange mechanism and the rapid decline when pH was approaching pK_a 2 indicates that cation exchange is no longer the dominant mechanism of adsorption (Wu *et al.* 2010). Despite the decrease, the continued adsorption of ciprofloxacin at pH ≥ pK_a 2 indicates that another mechanism is responsible for adsorption, possibly hydrogen bonding and/or hydrophobic interactions due to π–π stacking. It is also highly likely that ciprofloxacin and isoniazid can interact with the $Si\text{-}O^-$ and $Al\text{-}O^-$ functional groups on the surfaces of the adsorbents via complex formation and/or ion exchange. It is, therefore, important to note that although one mechanism dominates at certain pH, other mechanisms may also be involved adsorption process. The nitrogen and oxygen groups present in the structure of isoniazid enable it to form complexes with adsorbents as a ligand. The amino group hydrogens and carbonyl group oxygen of isoniazid are capable of forming hydrogen bonds with the adsorbents (Akyuz and Akyuz, 2008). Isoniazid is also amphoteric and has multiple ionizable groups. It speciates as a function of pH and has two pK_a values, pK_a 1 = 3.53 and is a result of the protonation of the heterocyclic nitrogen atom under acidic conditions. pK_a 2 = 11.40 and is ascribed to the proton loss from the amide nitrogen atom aggravated by basic conditions. At pH < 5, isoniazid exists as three species in equilibrium: one neutral and two positively charged. In the pH range 5 – 9, isoniazid has an uncharged molecular form. Deprotonation occurs gradually with increasing pH above 9 resulting in a negatively charged species (Blokhina *et al.* 2015).

As seen in Figs. 2 and 3 the high adsorption of isoniazid by kaolinite and perlite at pH 3 suggests that cation exchange is the main mechanism of adsorption and this is further confirmed by the drastic decline in adsorption when pH ≥ pK_a 1 of isoniazid since the cationic species is no longer dominating.

The invariance in adsorption of isoniazid exhibited by all the adsorbents in the pH range 5 – 10 suggests that mechanism of adsorption is consistent throughout the range and since isoniazid exists predominantly as a neutral species in this range adsorption is most likely attributed to hydrogen bonding and hydrophobic interactions between the isoniazid and adsorbents. The decrease in adsorption observed at pH ≥ 10 is most likely due to electrostatic repulsion between the negatively charged isoniazid species and the highly negative surface charge of the adsorbent. Interestingly, the adsorption capacities were relatively stable throughout the entire pH range when FA was used as an adsorbent for both ciprofloxacin and isoniazid, indicating that pH had no significant influence on adsorption. This shows that FA has excellent environmental adaptability. Therefore, in contrast to the other adsorbents, hydrophobic interactions are probably more important than electrostatic forces in the adsorption of ciprofloxacin and isoniazid by FA. The pyridine ring of isoniazid probably makes it capable of forming hydrophobic bonds especially when

the cyclic nitrogen forms a hydrogen bond the rest of the ring becomes more electronegative. The aromatic ring found in ciprofloxacin is also rich in delocalised electrons.

Effect of initial antibiotic concentration

The effect of initial antibiotic concentration on the removal of ciprofloxacin and isoniazid by the adsorbents is presented in Fig. 3. The amount of both ciprofloxacin and isoniazid adsorbed increases with increase in initial antibiotic concentration, which is most probably due to increasing concentration gradient of the antibiotic between the solution and adsorbent particles, resulting in a greater driving force of the mass transfer of the antibiotic molecules from the bulk solution to the solid phase (Singh *et al.* 2016). However, it is evident that the percentage of antibiotic removed decreases with increase in initial antibiotic concentration. This is because at lower antibiotic concentrations, the ratio of the initial number of antibiotic molecules/ions to the available surface area of adsorbent is larger, and vice versa (Nithya *et al.* 2016). Kaolinite removed all ciprofloxacin to concentrations below the detection limit for ciprofloxacin solutions which had an initial concentration less than 50 mg/L. The removal percentages of the ciprofloxacin after shaking for 30 min increased in the order FA < perlite < talc < vermiculite < kaolinite while those of isoniazid increased in the order vermiculite < talc < perlite < FA < kaolinite. The order remained the same despite the change in initial antibiotic concentrations.

Effect the solid/liquid ratio on antibiotic sorption

The adsorption of ciprofloxacin and isoniazid was studied by varying the solid/liquid ratio by adjusting the adsorbent dosage from 0.10 to 0.25 g and 0.5 to 1.5 g, respectively while keeping other parameters constant. It is clear that an increase in the solid/liquid ratio results in a greater percentage removal due to increased contact between the the solute molecules and the adsorbent However, it is more interesting to note that the amount of antibiotic loaded per unit adsorbent at equilibrium tends to decrease with increase in the solid/liquid ratio. This is because at higher doses aggregation of the adsorbent particles may occur resulting in a reduction of freely accessible sorption sites for the solute (Nithya *et al.* 2016). Hence, the adsorption capacity of adsorbent is not fully utilised.

Adsorption isotherms

The reason for employing adsorption isotherms was to analyse the relationship between the equilibrium concentration of antibiotic in solution and the amount adsorbed at the adsorbents surface. Furthermore, adsorption isotherms provide constant values which enable us to compare the adsorption capacities for different adsorbents for ciprofloxacin and isoniazid. The linearised plots of the Langmuir (Eq. 6), Freundlich (Eq. 7) and Temkin (Eq. 8) adsorption isotherms were used to analyse the

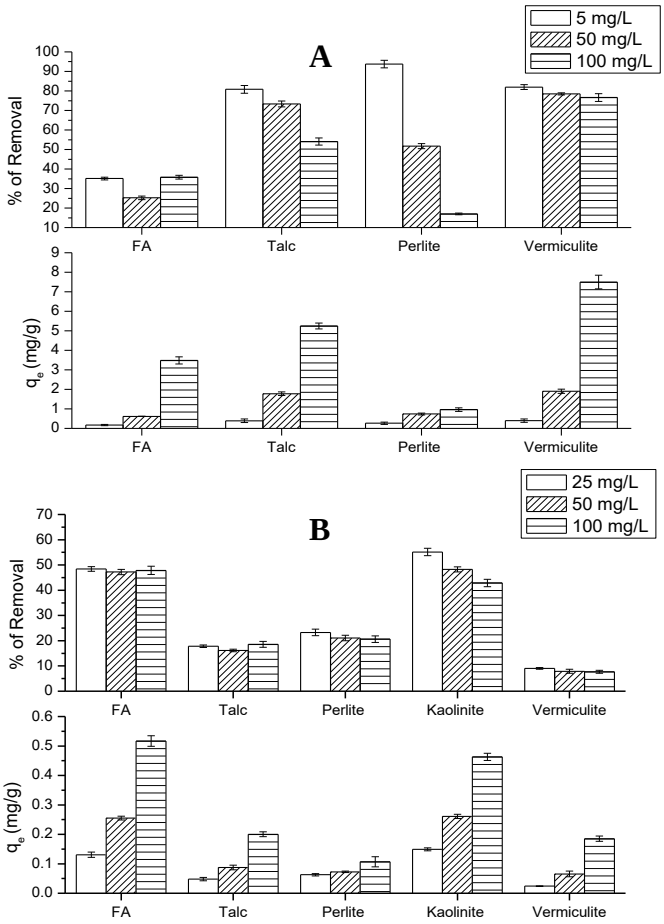

Fig. 3. Effect of initial antibiotic concentration on the adsorption of (A) ciprofloxacin and (B) isoniazid onto FA, perlite, talc, vermiculite and (B) isoniazid onto FA, kaolinite, perlite, talc and vermiculite. % removal and amount adsorbed at equilibrium (q_e) presented as the mean ± standard deviation (n = 3).

Table 4. Adsorption isotherm constants and correlation coefficients for adsorption of ciprofloxacin onto FA, kaolinite, perlite, talc and vermiculite.

	Langmuir			Freundlich			Temkin		
Adsorbent	K_l [L/mg]	q_m [mg/g]	R^2	$1/n$	K_f [mg/g]	R^2	K_t [L/mg]	B [J/mol]	R^2
FA	0.017	3.123	0.989	0.942	0.051	0.960	$e^{-1.494}$	0.927	0.694
Talc	0.064	6.083	0.998	0.667	0.436	0.993	$e^{-0.035}$	1.215	0.928
Perlite	1.505	0.819	0.978	0.221	0.392	0.953	$e^{3.478}$	0.122	0.997
Kaolinite	0.002	500.0	0.995	0.993	0.778	0.992	$e^{-1.427}$	10.460	0.930
Vermiculite	0.039	11.93	0.998	0.901	0.115	0.999	$e^{-0.245}$	2.056	0.826

experimental data. The regression line correlation coefficients (R^2) of the plots were used to establish the model which best described the data.

$$\frac{1}{q_e} = \frac{1}{q_m} + \frac{1}{K_l C_e q_m} \quad (6)$$

$$ln\, q_e = ln\, K_f + \frac{1}{n} ln\, C_e \quad (7)$$

$$q_e = B\, ln\, K_t + B\, ln\, C_e \quad (8)$$

In Eq. 6, 7 and 8, q_e is the equilibrium adsorption capacity of the adsorbent, i.e. the equilibrium solid phase/sorbed concentration of the antibiotic in question (mg/g), C_e is the concentration of antibiotic in the aqueous phase at equilibrium. The term of q_m (mg/g) is the equilibrium solid phase/sorbed concentration of the antibiotic in question required to achieve monolayer coverage of the adsorbent surface (mg/g). At the same time, q_m and K_l (sorption coefficient for the antibioti in question; L/mg) are adjustable parameters of Langmuir isotherm. K_f (mg/g) and n are Freundlich parameters representing the adsorption constant and the adsorption intensity, respectively. K_t (L/g) is the Temkin isotherm equilibrium binding constant and B (J/mol) is the Temkin's heat of adsorption (Can *et al.* 2016). The adsorption isotherm parameters and R^2 values obtained from fitting the experimental data obtained at 25±1 °C to linear plots of the isotherms values are presented in Table 4 and Table 5.

In order to quantify the applicability of the isotherm models, the R^2 values were used. These revealed that the Langmuir model was the best fit for the sorption of ciprofloxacin onto FA, talc and kaolinite with $R^2 \geq 0.99$, which implies that adsorption was predominantly a monolayer physical process. The Freundlich and Temkin isotherms gave the best for the sorption of ciprofloxacin onto vermiculite and perlite, respectively both with $R^2 \geq 0.99$. The Langmuir isotherm also gave the best fit for the adsorption of isoniazid onto FA, talc, perlite and vermiculite exhibiting R^2 values in the range 0.90 – 0.99, the Freundlich isotherm was the better fit for the sorption of isoniazid onto kaolinite with $R^2 \geq 0.99$. The Freundlich model mainly describes adsorption onto surfaces with no uniform energy distribution which means the adsorption is heterogeneous (Guan *et al.* 2017). However, R^2 values only give us an indication of the degree to which the experimental data agree with each other. It is, therefore, important to also take into account the isotherm parameters when assessing the applicability of an isotherm.

The Freundlich constant, *1/n* is a function of the strength of adsorption in the adsorption process and ideally, it should have a value less than one during a normal adsorption process which is an indication that the adsorption sites are homogenous in energy and there is no interaction between the adsorbed species. When *1/n* assumes a value greater than 1, the interactions become weak and adsorption becomes unfavourable (Can *et al.* 2016). The values of the Freundlich exponent, *1/n*, range from 0.221 – 0.998, indicating a favourable adsorption of ciprofloxacin and isoniazid onto the adsorbents.

The heat of sorption, *B*, calculated from the Temkin plots has values ranging between 0.018 – 10.460 J/mol, indicating a physical adsorption process (physisorption). Unlike the Langmuir and Freundlich isotherm models, the Temkin isotherm takes into account the interactions between adsorbents and antibiotics in solution which is based on the assumption that the free energy of adsorption is simply a function of surface coverage (Abdelnaeim *et al.* 2016). Again, looking,

Table 5. Adsorption isotherm constants and correlation coefficients for adsorption of isoniazid onto FA, kaolinite, perlite, talc and vermiculite.

	Langmuir			Freundlich			Temkin		
Adsorbent	K_l x 10^{-3} [L/mg]	q_m [mg/g]	R^2	*1/n*	K_f x 10^{-3} [mg/g]	R^2	K_t [L/mg]	*B* [J/mol]	R^2
FA	1.134	7.092	0.999	0.983	9.727	0.998	$e^{-2.245}$	0.2752	0.953
Talc	0.879	2.481	0.990	0.998	1.973	0.987	$e^{-2.776}$	0.1098	0.917
Perlite	45.910	0.130	0.986	0.319	2.488	0.923	$e^{-0.502}$	0.0259	0.948
Kaolinite	18.002	0.824	0.994	0.697	25.991	0.999	$e^{-1.804}$	0.1925	0.968
Vermiculite	15.365	0.099	0.908	0.486	0.619	0.775	$e^{-1.557}$	0.0183	0.790

at the regression R^2 values obtained (0.694 – 0.997), this isotherm is applicable to the description of majority data equilibrium data and gave the best fit for the adsorption of ciprofloxacin by perlite. Comparing the isotherms applied, the Langmuir gave the best fit, followed by the Freundlich isotherm and the least fit was obtained from the Temkin isotherm model. Kaolinite exhibited the greatest removals of both ciprofloxacin and isoniazid from aqueous solutions, achieving removals of up to 99 % and 55 %, respectively. The results indicate that the adsorption of ciprofloxacin and isoniazid mainly by surface coverage of the adsorbents and this corresponds with the findings from the kinetic studies which revealed that adsorption was mainly controlled external mass transfer.

Conclusions

This work presented the feasibility of adsorption of ciprofloxacin and isoniazid using FA, kaolinite, perlite, talc and vermiculite. The adsorbents were used without any chemical modification and can therefore significantly cut costs for wastewater treatment. All adsorbents except FA showed excellent adsorption of ciprofloxacin from aqueous solutions with all of them achieving removals ranging from 80 % – 99 %. The adsorbents were less efficient in removing isoniazid and kaolinite gave the highest removal of 55 %. The pH plays an important role in the adsorption process by affecting the surface charge of the adsorbent, the degree of ionisation and speciation of the adsorbate.. Adsorption kinetics data were described by the pseudo-second-order equation and application of the intraparticle diffusion model revealed that the adsorption processes were not only controlled by intra-particle diffusion. Both the Langmuir and Freundlich isotherms were applicable to the equilibrium data, indicating that the adsorption processes were spontaneous and exothermic.

References

Abdelnaeim MY, El Sherif IY, Attia AA, Fathy NA, El-Shahat MF (2016) Impact of chemical activation on the adsorption performance of common reed towards Cu(II) and Cd(II). Int. J. Miner. Process. 157: 80-88.

Ahmaruzzaman M (2010) A review on the utilization of fly ash. Prog. Energy Combust. Sci. 36: 327-363.

Akyuz S, Akyuz T (2008) FT-IR and FT-Raman spectroscopic studies of adsorption of isoniazid by montmorillonite and saponite. *In* Vib. Spectrosc., A collection of papers presented at the 4th International Conference on Advanced Vibrational Spectroscopy (ICAVS-4) Corfu, Greece, 10-15 June 2007 - Part II., 48.

Akyuz S, Akyuz T, Akalin E (2010) Adsorption of isoniazid onto sepiolite–palygorskite group of clays: An IR study. Spectrochim. Acta. A. Mol. Biomol. Spectrosc. 75: 1304-1307.

Alkan M, Karadaş M, Doğan M, Demirbaş Ö (2005) Adsorption of CTAB onto perlite samples from aqueous solutions. J. Colloid Interface Sci. 291: 309-318.

Bengtsson-Palme J, Larsson DGJ (2016) Concentrations of antibiotics predicted to select for resistant bacteria: Proposed limits for environmental regulation. Environ. Int. 86: 140-149.

Blokhina SV, Ol'khovich MV, Sharapova AV, Volkova TV, Perlovich GL (2015) Solution thermodynamics of pyrazinamide, isoniazid, and p-aminobenzoic acid in buffers and octanol. J. Chem. Thermodyn. 91: 396-403.

Böke N, Birch GD, Nyale SM, Petrik LF (2015) New synthesis method for the production of coal fly ash-based foamed geopolymers. Constr. Build. Mater. 75: 189-199.

Can N, Ömür BC, Altındal A (2016) Modeling of heavy metal ion adsorption isotherms onto metallophthalocyanine film. Sens. Actuators B Chem. 237: 953-961.

Castrillo PD, Olmos D, González-Benito J (2015) Kinetic study of the intercalation process of dimethylsulfoxide in kaolinite. Int. J. Miner. Process. 144: 70-74.

Chang P-H, Jiang W-T, Li Z, Kuo C-Y, Wu Q, Jean J-S, Lv G (2016) Interaction of ciprofloxacin and probe compounds with palygorskite PFl-1. J. Hazard. Mater. 303, 55-63.

Chen J, Wei X-D, Liu Y-S, Ying G-G, Liu S-S, He L-Y, Su H-C, Hu L-X, Chen F-R, Yang Y-Q (2016) Removal of antibiotics and antibiotic resistance genes from domestic sewage by constructed wetlands: Optimization of wetland substrates and hydraulic loading. Sci. Total Environ. 565: 240-248.

Dellisanti F, Valdrè G, Mondonico M (2009) Changes of the main physical and technological properties of talc due to mechanical strain. Appl. Clay Sci. 42: 398-404.

Guan Z, Tang X-Y, Nishimura T, Huang Y-M, Reid BJ (2017) Adsorption of linear alkylbenzene sulfonates on carboxyl modified multi-walled carbon nanotubes. J. Hazard. Mater. 322: 205-214.

Hongo T, Yoshino S, Yamazaki A, Yamasaki A, Satokawa S (2012) Mechanochemical treatment of vermiculite in vibration milling and its effect on lead (II) adsorption ability. Appl. Clay Sci. 70: 74-78.

Kolvari E, Koukabi N, Hosseini MM (2015) Perlite: A cheap natural support for immobilization of sulfonic acid as a heterogeneous solid acid catalyst for the heterocyclic multicomponent reaction. J. Mol. Catal. Chem. 397: 68-75.

Koshy N, Singh DN (2016) Fly ash zeolites for water treatment applications. J. Environ. Chem. Eng. 4: 1460-1472.

Król M, Minkiewicz J, Mozgawa W (2016) IR spectroscopy studies of zeolites in geopolymeric materials derived from kaolinite. J. Mol. Struct. 1126: 200-206.

Luo Y, Guo W, Ngo HH, Nghiem LD, Hai FI, Zhang J, Liang S, Wang XC (2014) A review on the occurrence of micropollutants in the aquatic environment and their fate and removal during wastewater treatment. Sci. Total Environ. 473-474: 619-641.

Nageswara Rao R, Venkateswarlu N, Narsimha R (2008) Determination of antibiotics in aquatic environment by solid-phase extraction followed by liquid chromatography–electrospray ionization mass spectrometry. J. Chromatogr. A 1187: 151-164.

Ngally Sabouang CJ, Mbey JA, Hatert F, Njopwouo D (2015) Talc-based cementitious products: Effect of talc calcination. J. Asian Ceram. Soc. 3: 360-367.

Nithya R, Gomathi T, Sudha PN, Venkatesan J, Anil S, Kim S-K (2016) Removal of Cr (VI) from aqueous solution using chitosan-g-poly(butyl acrylate)/silica gel nanocomposite. Int. J. Biol. Macromol. 87: 545-554.

Oliveira MFL, China AL, Oliveira MG, Leite MCAM (2015) Biocomposites based on *Ecobras matrix* and vermiculite. Mater. Lett. 158: 25-28.

Onutai S, Jiemsirilers S, Thavorniti P, Kobayashi T (2016) Fast microwave syntheses of fly ash based porous geopolymers in the presence of high alkali concentration. Ceram. Int. 42: 9866-9874.

Ouchiar S, Stoclet G, Cabaret C, Georges E, Smith A, Martias C, Addad A, Gloaguen V (2015) Comparison of the influence of talc and kaolinite as inorganic fillers on morphology, structure and thermomechanical properties of polylactide based composites. Appl. Clay Sci. 116-117: 231–240.

Ràfols C, Bosch E, Ruiz R, Box KJ, Reis M, Ventura C, Santos S, Araújo ME, Martins F (2012) Acidity and hydrophobicity of several new potential antitubercular drugs: isoniazid and benzimidazole derivatives. J. Chem. Eng. Data 57: 330-338.

Rashad AM (2016a). Vermiculite as a construction material – A short guide for civil engineer. Constr. Build. Mater. 125: 53-62.

Rashad AM (2016b) A synopsis about perlite as building material – A best practice guide for civil engineer. Constr. Build. Mater. 121: 338-353.

Salehi MH, Beni OH, Harchegani HB, Borujeni IE, Motaghian HR (2011) Refining soil organic matter determination by loss-on-ignition. Pedosphere 21: 473-482.

Shearer CR, Provis JL, Bernal SA, Kurtis KE (2016) Alkali-activation potential of biomass-coal co-fired fly ash. Cem. Concr. Compos. 73: 62-74.

Simonin J-P (2016) On the comparison of pseudo-first order and pseudo-second order rate laws in the modeling of adsorption kinetics. Chem. Eng. J. 300: 254-263.

Singh H, Choden S (2014) Comparison of adsorption behaviour and kinetic modeling of bio-waste materials using basic dye as adsorbate. Indian J. Chem. Technol. 21: 359-367.

Singh M, Dosanjh HS, Singh H (2016) Surface modified spinel cobalt ferrite nanoparticles for cationic dye removal: Kinetics and thermodynamics studies. J. Water Process Eng. 11: 152-161.

Spence A, Kelleher BP (2012) FT-IR spectroscopic analysis of kaolinite–microbial interactions. Vib. Spectrosc. 61: 151-155.

Sprynskyy M, Kowalkowski T, Tutu H, Cukrowska EM, Buszewski B (2011) Adsorption performance of talc for uranium removal from aqueous solution. Chem. Eng. J., Special Section: Symposium on Post-Combustion Carbon Dioxide Capture 171: 1185-1193.

Sun D, Wang L (2015) Utilization of paraffin/expanded perlite materials to improve mechanical and thermal properties of cement mortar. Constr. Build. Mater. 101, Part 1: 791-796.

Sutcu M (2015) Influence of expanded vermiculite on physical properties and thermal conductivity of clay bricks. Ceram. Int. 41: 2819-2827.

Tandlich R, Balaz S (2011) Biphenyl sorption to different soil clay minerals. Afr. J. Agric. Res. 6: 2321-2328.

Tekin N, Dinçer A, Demirbaş Ö, Alkan M (2010) Adsorption of cationic polyacrylamide (C-PAM) on expanded perlite. Appl. Clay Sci. 50: 125-129.

Tian W, Kong X, Jiang M, Lei X, Duan X (2016) Hierarchical layered double hydroxide epitaxially grown on vermiculite for Cr(VI) removal. Mater. Lett. 175: 110-113.

Timakul P, Rattanaprasit W, Aungkavattana P (2016) Improving compressive strength of fly ash-based geopolymer composites by basalt fibers addition. Ceram. Int. 42: 6288-6295.

Tran L, Wu P, Zhu Y, Liu S, Zhu N (2015) Comparative study of Hg(II) adsorption by thiol- and hydroxyl-containing bifunctional montmorillonite and vermiculite. Appl. Surf. Sci. 356: 91-101.

ul Haq E, Kunjalukkal Padmanabhan S, Licciulli A (2014) Synthesis and characteristics of fly ash and bottom ash based geopolymers – A comparative study. Ceram. Int. 40: 2965-2971.

Visa M (2016) Synthesis and characterization of new zeolite materials obtained from fly ash for heavy metals removal in advanced wastewater treatment. Powder Technol. 294: 338-347.

Wei T, Zheng B, Liu J, Gao Y, Guo W (2014) Structures and thermal properties of fatty acid/expanded perlite composites as form-stable phase change materials. Energy Build. 68: 587-592.

Wu M-H, Que C-J, Xu G, Sun Y-F, Ma J, Xu H, Sun R, Tang L (2016) Occurrence, fate and interrelation of selected antibiotics in sewage treatment plants and their receiving surface water. Ecotoxicol. Environ. Saf. 132: 132-139.

Yao L, Wang Y, Tong L, Li Y, Deng Y, Guo W, Gan Y (2015) Seasonal variation of antibiotics concentration in the aquatic environment: a case study at Jianghan Plain, central China. Sci. Total Environ. 527-528: 56-64.

Yu F, Sun S, Han S, Zheng J, Ma J (2016) Adsorption removal of ciprofloxacin by multi-walled carbon nanotubes with different oxygen contents from aqueous solutions. Chem. Eng. J. 285: 588-595.

Zhang C, Zhang Z, Tan Y, Zhong M (2017) The effect of citric acid on the kaolin activation and mullite formation. Ceram. Int. 43: 1466-1471.

Zhao H, Liu X, Cao Z, Zhan Y, Shi X, Yang Y, Zhou J, Xu J (2016) Adsorption behavior and mechanism of chloramphenicols, sulfonamides, and non-antibiotic pharmaceuticals on multi-walled carbon nanotubes. J. Hazard. Mater. 310: 235-245.

Zhu X, Zhu Z, Lei X, Yan C (2016) Defects in structure as the sources of the surface charges of kaolinite. Appl. Clay Sci. 124-125: 127-136.